Chapter 13

MODE COUPLING

As the beam intensity increases, the shift of each longitudinal azimuthal mode becomes so big that two adjacent modes overlap each other. When this happens, the longitudinal azimuthal mode number m is no longer a good eigennumber, and we can no longer represent the perturbation distribution ψ_1 as a single azimuthal mode. Instead, ψ_1 should be represented by a linear combination of all azimuthal modes. This phenomenon has been referred to as "mode mixing," "mode coupling," "strong head-tail," and "transverse or longitudinal turbulence."

13.1 Transverse

Let us first consider transverse instability driven by a broadband impedance. This implies a single-bunch mechanism. We also set the chromaticity to zero. For the mth azimuthal mode and kth radial mode, Eq. (10.33) or (11.1) becomes

$$(\Omega - \omega_\beta - m\omega_s)\delta_{mm'}\delta_{kk'} = M_{mm'kk'} \tag{13.1}$$

where, with the aid of Eq. (10.33), the matrix M is defined as

$$M_{mm'kk'} = -\frac{ieI_b c}{2\omega_\beta E_0 \tau_L} \frac{\int d\omega Z_1^\perp(\omega)\tilde{\lambda}_{m'k'}(\omega)\tilde{\lambda}^*_{mk}(\omega)}{\int d\omega \tilde{\lambda}_{mk}(\omega)\tilde{\lambda}^*_{mk}(\omega)} \ . \tag{13.2}$$

The summations have been converted to integrations because the impedance is so broadband that there is no need to distinguish the individual betatron lines. A further sim-

plification is to keep only the first most easily excited radial modes. Then, the problem becomes coupling in the azimuthal modes.

Since $\mathcal{R}e\, Z_1^\perp(\omega)$ is odd in ω and $\mathcal{I}m\, Z_1^\perp(\omega)$ is even in ω, only $\mathcal{I}m\, Z_1^\perp(\omega)$ will contribute to the diagonal terms of the matrix M giving only real frequency shifts which will not lead to instability. As the beam current becomes larger, two modes will collide and merge together, resulting in two complex eigenfrequencies, one is the complex conjugate of the other, thus introducing instability. Therefore, coupling should originate from the off-diagonal elements closest to the diagonal. We learn from Eq. (10.41) that the mth mode of excitation $\tilde{\lambda}_m(\omega)$ is even in ω when m is even, and odd in ω when m is odd. Thus, it is $\mathcal{R}e\, Z_1^\perp(\omega)$ that gives the coupling.

The eigenfrequencies are solved by

$$\det[(\Omega - \omega_\beta - m\omega_s)I - M] = 0 \ . \tag{13.3}$$

We recall Eq. (10.21), Sacherer integral equation for transverse instability in Chapter 10,

$$(\Omega - \omega_\beta - m\omega_s)\alpha_m R_m(r) = \\ -\frac{i\pi e^2 MNc}{E_0\omega_\beta T_0^2}\, g_0(r) \sum_{m'} i^{m-m'}\alpha_{m'} \int r'dr' R_{m'}(r') \sum_q Z_1^\perp(\omega_q) J_{m'}(\omega_q r') J_m(\omega_q r) \ , \tag{13.4}$$

where $g_0(r)$ is the unperturbed normalized distribution in the longitudinal phase space in circular coordinate. Clearly the equation is solvable if $g_0(r)$ is a δ-function. This is the air-bag model with beam particles residing only at the outer edge or $g_0(r) \propto \delta(r - \hat{\tau})$ with $\hat{\tau}$ representing the half length of the bunch.

Let us choose a simple transverse wake which is a constant W_1. The corresponding transverse impedance is

$$Z_1^\perp(\omega) = \frac{W_1}{\omega + i\epsilon} = \wp\left(\frac{W_1}{\omega}\right) - i\pi W_1 \delta(\omega) \ . \tag{13.5}$$

The infinite matrix is truncated and the eigenvalues solved numerically. The solution is shown in Fig. 13.1 [2]. This impedance corresponds to a real part that falls off as frequency increases. The imaginary part is a δ-function at zero frequency, and therefore interacts with the $m = 0$ mode only, since all $m \neq 0$ modes have spectral distribution $\tilde{\lambda}_m(0) = 0$. This explains why all other modes remain almost unshifted with the exception of $m = 0$. The downward frequency shift of the $m = 0$ mode as the beam intensity increases from zero is a general behavior for short bunches. The transverse wake force

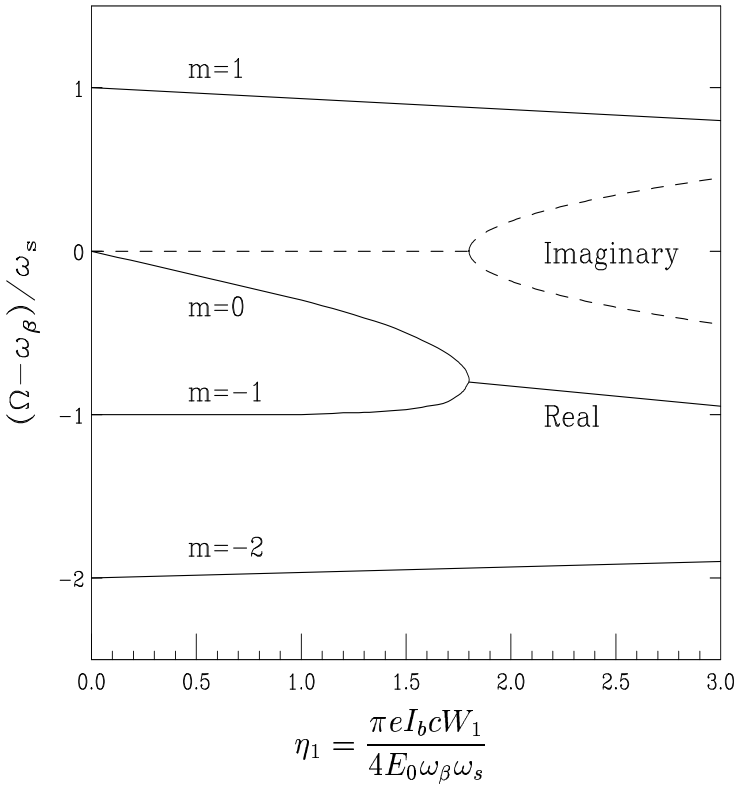

Figure 13.1: Transverse mode frequencies $(\Omega - \omega_\beta)/\omega_s$ versus the current intensity parameter η_1 for an air-bag bunch distribution perturbed by a constant wake potential W_1. The instability occurs at $\eta_1 \approx 1.8$, when the $m = 0$ and $m = -1$ modes collide. The dashed curves are the imaginary part of the mode frequencies or growth/damping rate for the two colliding modes.

produced by an off-axis beam has the polarity that deflects the beam further away from the pipe axis. This force acts as a defocusing force for the rigid beam mode, and therefore the frequency shifts downward. Such a downshift of the betatron frequency is routinely observed in electron accelerators and serves as an important tool of probing the impedance. Notice that unlike the situation of the longitudinal mode coupling described in Chapter 7 and later in this chapter, there is no symmetry of the azimuthal modes about the $m = 0$ mode. This is because these are now sidebands of the betatron lines, and the betatron lines do not have any symmetry about the zero frequency. The implication is that we need to include both positive and negative azimuthals in the discussion.

Eventually the $m = 0$ shifts downwards and meets with the $m = -1$ mode, thus

exciting an instability. The threshold is at

$$\eta_1 = \frac{\pi e I_b c W_1}{4 E_0 \omega_\beta \omega_s} \approx 1.8 \ , \tag{13.6}$$

and is bunch-length independent. We can also obtain an approximate threshold from Eqs. (13.1) and (13.2) by equating the frequency shift to ω_s, and get

$$\frac{e I_b c \ Z_1^\perp\big|_{\rm eff}}{2 E_0 \omega_\beta \omega_s \tau_{\scriptscriptstyle L}} \approx 1 \ , \tag{13.7}$$

where

$$Z_1^\perp\big|_{\rm eff} = \frac{\displaystyle\int d\omega Z_1^\perp(\omega) h_m(\omega)}{\displaystyle\int d\omega h_m(\omega)} \tag{13.8}$$

is called the *effective transverse impedance* for mode m. Comparing Eqs. (13.6) and (13.7), we find the two thresholds are almost the same except for the bunch-length dependency, which we think should be understood as follows. The imaginary part of the impedance in Eq. (13.5) is a δ-function at zero frequency which interacts only with the $m = 0$ mode. As the bunch length becomes shorter, the spectrum spreads out wider, so that the spectrum at zero frequency becomes smaller, and $Z_1^\perp\big|_{\rm eff}$ is also smaller accordingly. In fact, from Eq. (10.43), the normalization of the power spectrum in the denominator of Eq. (13.8) is just $\tau_{\scriptscriptstyle L}^{-1}$ and from Eq. (10.42), $h(0)$ is $\tau_{\scriptscriptstyle L}$ independent. It is clear that $Z_1^\perp\big|_{\rm eff} \propto \tau_{\scriptscriptstyle L}$, thus explaining why η_1 in Eq. (13.6) is bunch-length independent.

Now consider the situation when the impedance is a broadband resonance. For a very short bunch, the $m = 0$ mode extends to very high frequencies and will cover part of the high-frequency capacitive part of the resonance. Thus, the effective impedance $Z_1^\perp\big|_{\rm eff}$ can become small due to the cancellation of the inductive and capacitive parts. At the same time, the peak of $\mathcal{R}e\, Z_1^\perp$ is far from the peak of the $m = -1$ mode, thus making the coupling between the $m = 0$ and $m = -1$ mode very weak. Since the frequency shift is small and the coupling is weak, it will take a much higher beam current for the $m = 0$ mode to meet with the $m = -1$ mode, thus pushing up the threshold current. For a long bunch, the $m = 0$ mode has a small frequency spread. If it stays inside the inductive region where $\mathcal{I}m\, Z_1^\perp$ is almost constant, $\mathcal{I}m\, Z_1^\perp$ can be taken out of the integral and $Z_1^\perp\big|_{\rm eff}$ will be almost constant. Therefore, the threshold current, given by Eq. (13.7), increases linearly with the bunch length. When the bunch is very long, the $m = \pm 1$ and even $m = \pm 2$ and $m = \pm 3$ modes may stay inside the constant inductive region of the

impedance. This implies that the higher azimuthal modes also interact strongly with the impedance and these modes will have large shifts so that the threshold can become much smaller. Several collisions may occur around a small beam-current interval and the bunch can become very unstable suddenly.

The transverse mode-coupling instability was first observed at the DESY PETRA and later also at the SLAC PEP and the CERN LEP. The strong head-tail instability is one of the cleanest instabilities to observe in electron storage rings [1]. In particular, one may measure the threshold beam intensity when the beam becomes unstable transversely. Another approach is to measure the betatron frequency as the beam intensity is varied. From the shift of the betatron frequency per unit intensity increase, the transverse wake can be inferred. The transverse motion of the bunch across its length can also be observed easily using a streak camera.

In the longitudinal mode-mixing instability, the bunch lengthens as the beam becomes unstable essentially without losing beam particles. This does not happen in the transverse case. The instability is devastating; as soon as the threshold is reached, the bunch disappears. However, so far no strong head-tail instabilities have ever been observed in hadron machines.

Radiation damping is too slow to damp the strong head-tail instability. A damper significantly faster than the angular synchrotron frequency ω_s is required. As shown in Fig. 13.1, it is mode $m = 0$ that is shifted downward to collide with mode $m = -1$ so as to start the instability. But mode $m = 0$ is the pure rigid dipole betatron oscillation without longitudinal excitation. Therefore, if we can introduce a positive coherent betatron tune shift, it will slow this mode from coming down and therefore push the threshold to a higher value. A conventional feedback system is resistive; i.e., the kicker is located at an odd multiple of 90° from the pickup. Here, a reactive feedback system is preferred [2]. The kicker is located at an even multiple of 90° from the pickup. In a two-particle model, where the bunch is represented by two macro-particles, the equations of motion are, in the first half of the synchrotron period,

$$\begin{aligned} \frac{d^2y_1}{dn^2} + (2\pi\nu_\beta)^2 y_1 &= \sigma(y_1 + y_2) \ , \\ \frac{d^2y_2}{dn^2} + (2\pi\nu_\beta)^2 y_2 &= \sigma(y_1 + y_2) + \alpha y_1 \ , \end{aligned} \tag{13.9}$$

where y_1 and y_2 are, respectively, the transverse displacements of the head and tail macro-particles, σ is the gain of the reactive feed back, and α represents the effect of the

transverse wake from head to tail. Notice that the reactive feedback acts on the center of the bunch and is in phase with the particle displacements. It therefore modifies ν_β by introducing a tune shift. The instability threshold can then be raised by properly choosing the feedback strength σ. In low-energy hadron machines, the space charge tune shift constitutes a natural reactive feedback system which tends to shift the $m = 0$ mode upwards. We shall study this in more detail in the next section.

This instability can also be damped by Balakin-Novokhatsky-Smirnov (BNS) damping [3], which delivers a betatron tune spread from the head of the bunch to the tail. This can be achieved by tilting the longitudinal phase space distribution of the bunch so that the tail has a lower energy relative to the head through chromaticity. Another method to implement BNS damping is to introduce a radio-frequency quadrupole magnet system, so that particles along the bunch will see a gradual shift in betatron tune.

13.2 Space Charge and Mode Coupling

It was reported in a recent paper of Blaskiewicz [4] that the space charge tune shift can strongly damp the transverse mode-coupling instability (TMCI), which is also known as strong head-tail instability. The investigation was made on the basis of particle tracking and the analytically solvable *square-well air-bag model* [5]. This is different from the air-bag model we used in the last section, although all the beam particles reside at the edge of the bunch. The formation of this model is sketched in Fig. 13.2. From a ring of particles in the longitudinal phase space on the left, the top semi-circle is stretched out and so is the lower semi-circle as illustrated in the right plot. The stretching continues until the top and lower semi-circles become two horizontal lines at energy offset $\pm\widehat{\Delta E}$. The lower one is described by the synchrotron phase ϕ from $-\pi$ to 0, while the upper one by ϕ from 0 to π for one synchrotron oscillation. Such a synchrotron oscillation requires, of course, a special rf potential. The bunch will be very long. The head is represented by $\phi = 0$ while the tail is represented by $\phi = \pm\pi$. We use the synchrotron phase ϕ and the energy offset ΔE as a set of variables for the description of the particle position in the longitudinal phase space. Although z remains the coordinate orthogonal to ΔE, the linear position of the particle can also be referenced by ϕ. The bunch particle distribution is given by

$$\psi(\phi, \Delta E) = \tfrac{1}{2}\rho(\phi)\left[\delta(\Delta E - \widehat{\Delta E}) + \delta(\Delta E + \widehat{\Delta E})\right] , \tag{13.10}$$

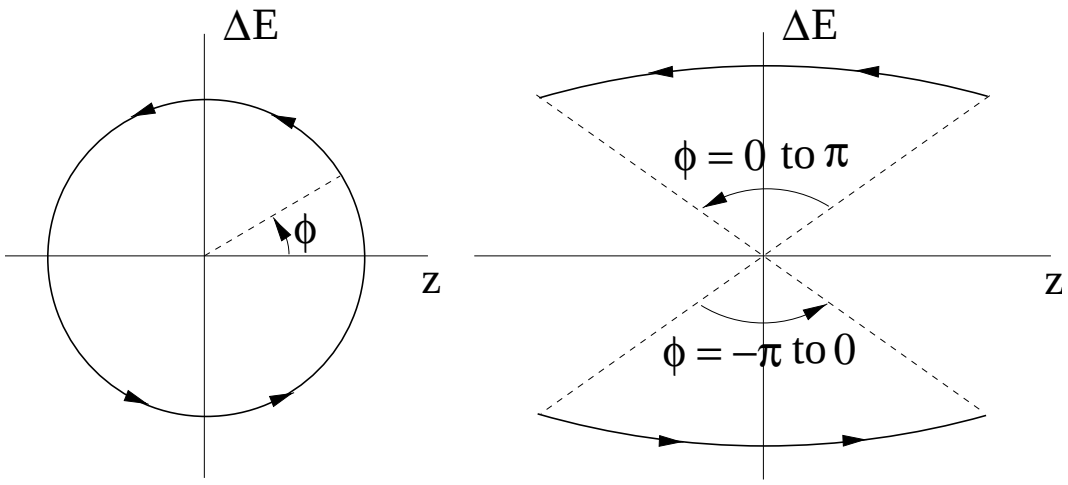

Figure 13.2: The ordinary air-bag model in the longitudinal phase space (left) is transformed into the square-well air-bag model (right) by stretching out the upper and lower semi circles until they become two infinite parallel lines at the energy spread $\pm\widehat{\Delta E}$. The longitudinal position of the particle remains specified by ϕ from $-\pi$ to 0 and from 0 to π.

where $\rho(\phi) = 1/(2\pi)$ is the projection onto the synchrotron phase.

What is going to be presented here is a qualitative explanation why the space charge helps TMCI. Without space charge, the bunch starts to be unstable when two neighboring synchro-betatron modes merge under the influence of the wake forces. Typically, the pure betatron mode (the azimuthal or synchrotron harmonic $m = 0$ mode, also known as the rigid-bunch mode) is affected by the wake force and shifts downward, while the other azimuthal modes are not much affected, at least at low intensity. The transverse wake force produced by an off-axis beam has the polarity that deflects the beam further away from the pipe axis. This force acts as a defocusing force for the rigid beam mode, and therefore the frequency shifts downward. As a result, the instability threshold is determined by the coupling of the 0 and -1 modes, as illustrated in the left plot of Fig. 13.3, (see below for definition of parameters).

The space charge by itself also shifts all the frequencies downward, as illustrated in the right plot of Fig. 13.3. The only exception is the azimuthal $m = 0$ mode, which describes the motion of the bunch as a whole, and, therefore, is not influenced by the space charge at all. Thus, in the presence of space charge, the $m = 0$ mode will couple with the $m = -1$ mode at a higher current intensity and therefore the threshold is raised

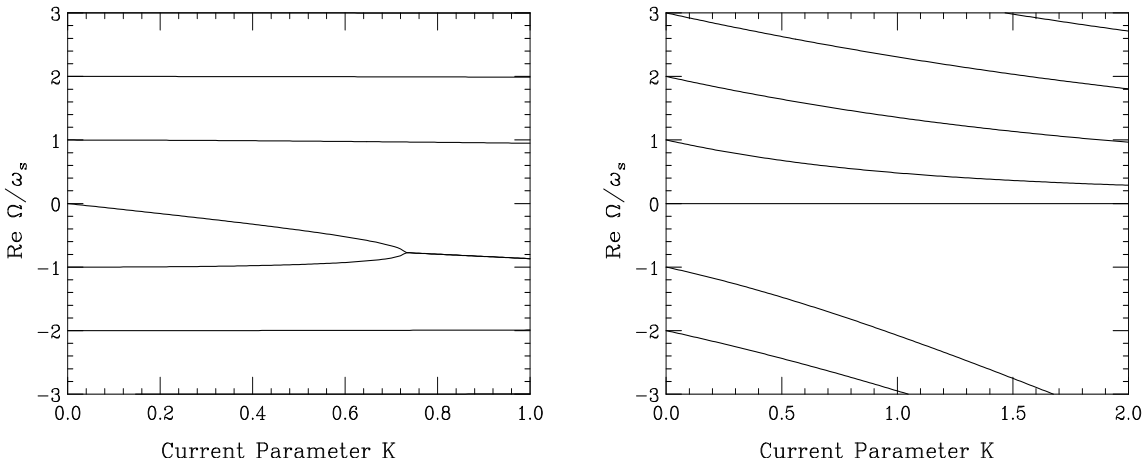

Figure 13.3: Left: The transverse wake force shifts mostly the azimuthal $m = 0$ mode downward but not the other modes. Instability occurs when the $m = 0$ and -1 modes meet with each other. Right: The space charge force in the absence of the wake forces shifts all modes downward with the exception of the $m = 0$ mode.

in the presence of space charge. This is illustrated in the left plot of Fig. 13.4.

Let us go in more details with mathematics. The transverse displacement $x(\phi)$ of a particle at the synchrotron phase ϕ satisfies the equation of motion:

$$\frac{d^2x(\phi)}{dt^2} + \omega_\beta^2 x(\phi) = F(\phi) + S\rho(\phi)[x(\phi) - \bar{x}(\phi)] \ , \tag{13.11}$$

where $\omega_\beta/(2\pi)$ is the unperturbed betatron frequency and the smooth approximation for the betatron oscillations has been applied. To incorporate synchrotron oscillation, the total time derivative takes the form

$$\frac{d}{dt} = \frac{\partial}{\partial t} + \omega_s \frac{\partial}{\partial \phi} \ , \tag{13.12}$$

with $\omega_s/(2\pi)$ being the synchrotron frequency. The right-hand side of Eq. (13.11) contains the transverse driving forces. The first term is the transverse wake force

$$F(\phi) = -\frac{N_b e^2 c^2}{E_0 C} \int_0^{|\phi|} W_1[z(\phi') - z(\phi)]\rho(\phi')\bar{x}(\phi')d\phi' \ , \tag{13.13}$$

where N_b is the number of particles in the bunch, W_1 the transverse wake function, $z(\phi)$ the longitudinal position of the beam particle. The second term is the space charge contribution. It is proportional to the linear density $\rho(\phi)$ and the displacement relative

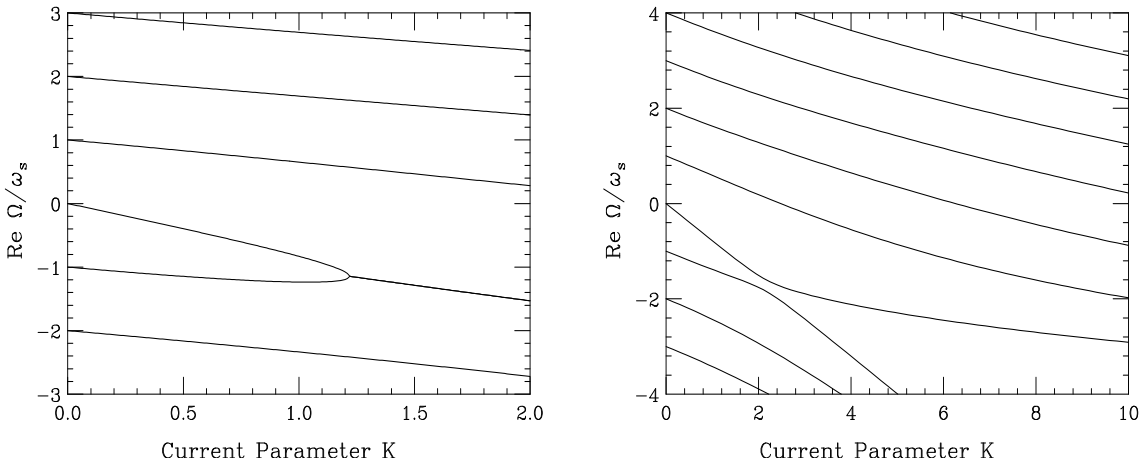

Figure 13.4: Left: With the transverse space charge force added to the wake forces, all modes except the $m = 0$ mode are shifted downward, thus requiring the $m = 0$ and -1 modes to couple at a much higher current threshold. Right: When space charge reaches the critical value of $\xi = 5$, the $m = -1$ mode is shifted away from the $m = 0$ mode by so much that they do not couple anymore.

to the local beam center, $x(\phi) - \bar{x}(\phi)$, with the constant S representing the space charge strength.

To solve the problem quantitatively, we expand the offset into the synchrotron harmonics (or azimuthals):

$$x(\phi, t) = e^{-i\omega_\beta t - i\Omega t} \sum_{n=-\infty}^{\infty} x_n e^{in\phi} \ , \tag{13.14}$$

where $\Omega/(2\pi)$ is the collective frequency shift. In this air-bag model, all particles reside at the edge of the bunch distribution in the longitudinal phase space. Note that because of the square-well air-bag model, these synchrotron azimuthals are slightly different from the conventional ones. The average offset at the synchrotron phase ϕ is therefore given by

$$\bar{x}(\phi, t) = \tfrac{1}{2}\Big[x(\phi, t) + x(-\phi, t)\Big] = e^{-i\omega_\beta t - i\Omega t} \sum_{n=-\infty}^{\infty} x_n \cos n\phi \ . \tag{13.15}$$

Following basically Ref. [6], Eq. (13.11) transforms into an eigenvalue equation,

$$\left(\frac{\Omega}{\omega_s} - n\right) x_n = -K \sum_{m=-\infty}^{\infty} x_m \big(\mathcal{W}_{nm} + \xi \mathcal{Q}_{nm}\big) \ . \tag{13.16}$$

Here, the current parameter is written as

$$K = \frac{N_b e^2 c^2 W_0}{2\pi^2 \omega_\beta \omega_s C E_0} \ . \tag{13.17}$$

The wake matrix elements are then given by

$$\mathcal{W}_{nm} = \int_0^\pi d\phi \int_0^\phi d\phi' w[z(\phi') - z(\phi)] \cos(n\phi) \cos(m\phi') \ , \tag{13.18}$$

where the wake function is presented as $W(z) = -W_0 w(z)$ with W_0 serving as a normalizing constant. The space charge parameter

$$\xi = \frac{\Delta\omega_\beta}{2K\omega_s} \tag{13.19}$$

is a current-dependent ratio of the incoherent tune shift

$$\Delta\omega_\beta = \frac{S\rho}{2\omega_\beta} \tag{13.20}$$

to the current parameter K. The space charge matrix elements are

$$\mathcal{Q}_{nm} = \delta_{nm} - \delta_{n,-m} \tag{13.21}$$

in the assumed air-bag distribution.

Without wake forces, the eigenvalue equation leads to the mode behavior presented in the right plot of Fig. 13.3. For the simplest step-like wake function $w(z) = H(z)$, $H(z)$ being the Heaviside step function, and without space charge ($\xi = 0$), the mode coupling is shown in the left plot of Fig. 13.3, where the threshold is $K = 0.73$. Now space charge is introduced with the space charge parameter $\xi = 4$. We do see in the left plot of Fig. 13.4 that, because the $m = -1$ mode is shifted downward by the space charge, the instability threshold has been pushed up to $K = 1.25$ as compared with the left plot of Fig. 13.3.

Further increasing the space charge parameter to $\xi = 5$, we see in the right plot of Fig. 13.4 that modes $m = 0$ and -1 do not merge any more. What is not shown in the plot is a much higher new threshold where the 0 mode couples with the $m = 1$ mode instead. This new threshold is very much model dependent. In the present model, it depends strongly on the number of modes included in the truncated matrix. For truncation at modes $|n| = 32$, this new threshold is at least a factor of 30 higher than

when space charge is absent. A dependence of the calculated threshold K_{th} on the mode truncation number $|n|$ was found as $K_{th} \propto |n|^{1/2}$ for $|n| \leq 10$ and even weaker,

$$K_{th} \propto |n|^{1/3} , \tag{13.22}$$

for $10 \leq |n| \leq 32$. The divergence is caused by the fact that the Fourier components of the space charge in Eq. (13.21) do not roll off at high frequencies. Taking into account the finite value of the ratio of transverse bunch size $\sigma_\perp$ to longitudinal bunch size $\sigma_\parallel$, we estimate this roll-off limit as $|n| \simeq \sigma_\perp/\sigma_\parallel \simeq 200$ to 1000 for typical hadron bunches. Extrapolation of the dependence Eq. (13.22) into this area brings to a conclusion that the actual threshold can be 2 to 3 times higher than the result reported for $|n| = 32$. So for this simplified wake-beam model, the space charge is found to be able to increase the TMCI threshold by one or two orders of magnitude.

As discussed in the previous section, a reactive feedback shifts mode $m = 0$ upwards resulting in pushing the threshold to a higher current. Here, the space charge force shifts all the modes downwards except $m = 0$, and the result is also to have the threshold pushed towards a higher current. Therefore, the space charge tune shift in a proton machine, as discussed above, constitutes a natural inverse reactive feedback.

13.3 Longitudinal

The azimuthal modes are not a good description of the collective motion of the bunch when the beam current is high enough. Therefore there is also mode coupling in the longitudinal motion. Similar to the transverse coupled problem in Eqs. (13.1) and (13.2), we have here

$$(\Omega - m\omega_s)\delta_{mm'}\delta_{kk'} = M_{mm'kk'} \tag{13.23}$$

where, with the aid of Eq. (10.37), the matrix M is defined as

$$M_{mm'kk'} = \frac{im}{1+m}\frac{4\pi^2 e I_b \eta}{3\beta^2 E_0 \omega_s \tau_L^3}\frac{\int d\omega \dfrac{Z_0^\parallel(\omega)}{\omega}\tilde{\lambda}_{m'k'}(\omega)\tilde{\lambda}^*_{mk}(\omega)}{\int d\omega \tilde{\lambda}_{mk}(\omega)\tilde{\lambda}^*_{mk}(\omega)} , \tag{13.24}$$

where the unperturbed distribution has been assumed to be parabolic. Again here the impedance is broadband so that the discrete summations over the synchrotron sidebands

have been replaced by integrals. We have also thrown away all the higher-order radial modes keeping the most easily excited $k = 1$. Exactly the same as in the transverse situation, only $\mathcal{I}m\, Z_0^{\parallel}(\omega)/\omega$ contributes to the diagonal elements of the coupling matrix and thus to the real frequency shifts of the modes. The coupling of two modes, mostly adjacent, will give instability, which is determined by $\mathcal{R}e\, Z_0^{\parallel}(\omega)/\omega$ in the off-diagonal elements next to the diagonal ones. All the discussions about bunch-length dependency on threshold in the transverse case apply here also. A rough estimate of the threshold can be obtained from Eq. (13.24) by equating the frequency shift to ω_s. The threshold is therefore

$$\eta_2 = \frac{4\pi^2 e I_b \eta}{3\beta^2 E_0 \omega_s^2 \tau_L^3} \left.\frac{Z_0^{\parallel}}{\omega}\right|_{\text{eff}} \approx 1 \ , \tag{13.25}$$

where the effective longitudinal impedance for mode m is defined as

$$\left.\frac{Z_0^{\parallel}}{\omega}\right|_{\text{eff}} = \frac{\displaystyle\int d\omega \frac{Z_0^{\parallel}(\omega)}{\omega} h_m(\omega)}{\displaystyle\int d\omega h_m(\omega)} \ , \tag{13.26}$$

For convenience, let us introduce a parameter $x = \omega\tau_L/\pi$, so that, with the exception of $m = 0$ which is not an allowed mode in the longitudinal motion, the mth mode of excitation peaks at $x \approx m{+}1$ and has a half width of $\Delta x \approx 1$. Now consider the Fermilab Main Ring with a revolution frequency 47.7 kHz and total bunch length $\tau_L \approx 2$ ns. Assume the impedance to be broadband centered at $x_r = 7.5$ or $f_r \sim 1.88$ GHz and quality factor $Q = 1$. Numerical diagonalization of the coupling matrix gives frequency shifts as shown in Fig. 13.5 [8]. We see the first instability occurs when mode $m = 6$ couples with mode $m = 7$, and in the vicinity of the threshold, there are also couplings between modes $m = 4$ and 5 and modes $m = 8$ and 9. This happens because the resonance centered at $x_r = 7.5$ has a half width $\Delta x_r = x_r/(2Q) = 3.75$. Thus the $\mathcal{R}e\, Z_0^{\parallel}/\omega$ resonant peak encompasses modes $m = 4$ to 9, which peak at $x = 5$ to 10. This is a typical picture of mode-coupling instability for long bunches. From the figure, the first instability occurs at

$$\epsilon = \frac{4\pi^2 e I_b \eta}{3\beta^2 E_0 \omega_s^2 \tau_L^3} \frac{R_s}{\omega_r} \approx 0.93 \ . \tag{13.27}$$

On the other hand, the Keil-Schnell criterion of Eq. (6.22) gives a threshold of

$$\frac{e I_b \eta}{\beta^2 E_0 \omega_s^2 \tau_L^3} \frac{R_s}{\omega_r} = \frac{1}{6\pi} \frac{1}{F} \ , \tag{13.28}$$

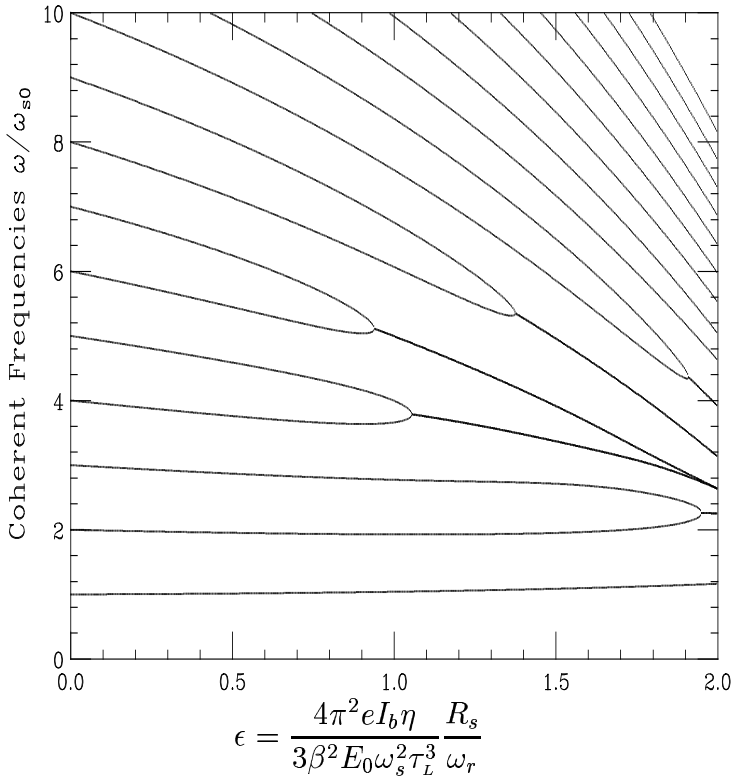

Figure 13.5: Coupling of modes $m = 6$ and 7 in the presence of a resonance at $x_r = 7.5$ and $Q = 1$ above transition.

where F is the form factor. This is equivalent to

$$\epsilon = \frac{2\pi}{9} \frac{1}{F} \ . \tag{13.29}$$

Thus, the mode-coupling threshold is very close to the Keil-Schnell threshold. However, mode-coupling instability is quite different from microwave instability. In the latter, pure reactive impedance can drive an instability; for example, the negative-mass instability just above transition is driven by the space charge force. It can be demonstrated that pure capacitive impedance will only lead to real frequency shifts of the modes. Although two modes may cross each other, they will not be degenerate to form complex modes. Thus, there is no instability (Exercise 13.2).

When the bunch is short, for example, electron bunches, the modes of excitation spread out to higher frequencies. Therefore when the bunch is short enough, the resonant peak of $\mathcal{R}e\, Z_0^{\parallel}/\omega$ will encompass only modes $m = 1$ and 2. Thus, we expect these two

modes will collide first to give instability. The $m = 1$ is the dipole mode and is not shifted at low beam current because the bunch center does not see any reactive impedance. The $m = 2$ is the quadrupole mode, which is shifted downward above transition. This downshift is a way to measure the reactive impedance of the ring.

When the beam current is above threshold and instability starts, the energy spread increases and so does the bunch length. In an electron ring where there is radiation damping, there is no overshooting and the increase stops when the stability criterion is fulfilled again. The bunch lengthening is therefore determined by the stability criterion. If the bunch samples the impedance at a frequency range where $Z_0^{\|}(\omega) \propto \omega^a$, the effective impedance is

$$\left.\frac{Z_0^{\|}}{\omega}\right|_{\rm eff} \propto \frac{\int d\omega\, \omega^{a-1} h_m(\omega)}{\int d\omega\, h_m(\omega)} \propto \tau_{_L}^{1-a} \ , \tag{13.30}$$

where use has been made of the fact that the power spectrum h_m is a function of the dimensionless quantity $\omega\tau_{_L}$ according to Eq. (10.42) and the result is independent of the functional form of h_m. From the threshold condition in Eq. (13.25), we have

$$\frac{4\pi^2 e I_b \eta}{3\beta^2 E_0 \omega_s^2 \tau_{_L}^{2+a}} = \text{constant independent of } I_b,\ \eta,\ E_0,\ \omega_s,\ \tau_{_L} \ . \tag{13.31}$$

Thus the bunch length obeys the scaling criterion of

$$\tau_{_L} \propto \xi^{1/(2+a)} \ , \tag{13.32}$$

where

$$\xi = \frac{\eta I_b}{\nu_s^2 E_0} \tag{13.33}$$

is the scaling parameter introduced by Chao and Gareyte [2].

Longitudinal mode coupling is different from transverse mode coupling. In the latter, the betatron frequency ($m = 0$) is shifted downward to meet with the $m = -1$ mode. The amount of shift is small, since $\nu_s/[\nu_\beta] \ll 1$, where $[\nu_\beta]$ is the residual betatron tune. Transverse mode coupling has been measured in many electron rings and the results agree with theory. In the longitudinal case, the synchrotron quadrupole frequency ($m = 2$) has to be shifted downward to meet with the synchrotron dipole frequency ($m = 1$) and this shift is 100% of the synchrotron tune. At the CERN LEP which is above transition, we expect the synchrotron quadrupole mode to shift downward

when the beam current increases from zero. However, it was observed that this mode shifts slightly upward instead. Since the dipole frequency is not shifted, it is hard to visualize how the two modes will be coupled. Some argue that the coupling may not be between two azimuthal modes, but instead between two radial modes that we have discarded in our discussion. But the coupling between two radial modes is generally much weaker. Some say that the actual coupling of the two modes has never been observed experimentally, and the scaling law for bunch lengthening may have been the result of some other theories. Anyway, the theory of longitudinal mode coupling is far from satisfactory.

13.4 High Energy Accelerators

So far transverse mode-coupling instability has never been observed in hadron machines. In this section, we would like to analyze how this instability would affect the higher energy accelerators under design.

For protons, particle energy E_0 is directly proportional to the size of the accelerator. So we have

$$E_0 \propto R \quad \text{and} \quad \omega_0 \propto \frac{1}{R} \,. \tag{13.34}$$

The resistive-wall impedance is

$$\frac{Z_0^{\parallel}}{n} = [1 - i\,\mathrm{sgn}(\omega)]\frac{R\rho}{nb}\sqrt{\frac{\mu\omega}{2\rho}} \,, \tag{13.35}$$

where ρ is the resistivity and μ the magnetic permeability of the beam pipe of radius b. At a fixed frequency ω, we have

$$\frac{Z_0^{\parallel}}{n} \sim \frac{1}{b\sqrt{\omega}} \,, \tag{13.36}$$

$$Z_1^{\perp} \sim \frac{R}{b^3\sqrt{\omega}} \,. \tag{13.37}$$

For M pairs of strip-line BPM's at low frequencies $\omega \lesssim c/\ell$, where ℓ is the length of the

strip lines,

$$\frac{\mathcal{I}m\, Z_0^{\parallel}}{n} = -i2MZ_c \left(\frac{\phi_0}{2\pi}\right)^2 \frac{\ell}{R} \ , \tag{13.38}$$

$$\mathcal{I}m\, Z_1^{\perp} = \frac{c}{2b^2}\left(\frac{4}{\phi_0}\right)^2 \sin^2\frac{\phi_0}{2}\frac{\mathcal{I}m\, Z_0^{\parallel}}{\omega} \ . \tag{13.39}$$

where Z_c is the characteristic impedance and ϕ_0/π is the fraction of the beam pipe covered by the strip lines. The betatron functions $\beta_{x,y}$ scale as $\sqrt{R}$. Thus, the betatron tunes and the number of BPM's required also scale as $\sqrt{R}$. At a fixed frequency we have

$$\frac{\mathcal{I}m\, Z_0^{\parallel}}{n} \sim \frac{\ell}{\sqrt{R}} \ , \tag{13.40}$$

$$\mathcal{I}m\, Z_1^{\perp} \sim \frac{\ell}{b^2}\sqrt{R} \ . \tag{13.41}$$

We see that when the size of an accelerator is increased, the resistive-wall impedance will dominate over all other contributions. We also see that $Z_0^{\parallel}/n$ at a fixed frequency remains roughly independent of the size of the accelerator. From now on, we will consider resistive-wall impedance only.

The Keil-Schnell criterion for longitudinal microwave instability is

$$\left|\frac{Z_0^{\parallel}}{n}\right| < \frac{2\pi|\eta|E_0\sigma_\delta^2}{eI_{\rm peak}} \ . \tag{13.42}$$

For a large accelerator, the energy is usually very much larger than the transition energy. The slip factor $\eta \sim \gamma_t^{-2} \sim \nu_\beta^{-2}$ for a FODO lattice. We therefore have $\eta \sim R^{-1}$. The peak current is $I_{\rm peak} \sim N_b/\sigma_\tau$. Putting in the wall resistivity at $\omega \sim \sigma_\tau^{-1}$, the stability criterion takes the form

$$\frac{\sqrt{\sigma_\tau}}{b} \lesssim \frac{A\sigma_\delta}{N_b R} \ , \tag{13.43}$$

where the bunch area in eV-s is

$$A = E_0\sigma_\delta\sigma_\tau \ . \tag{13.44}$$

For an accelerator of higher energy, if we want to have roughly the same fractional energy spread and bunch length, the bunch area will scale as R. The above stability criterion becomes

$$\frac{\sqrt{\sigma_\tau}}{b} \lesssim \frac{\sigma_\tau\sigma_\delta^2}{N_b} \ . \tag{13.45}$$

This leads to the conclusion that longitudinal microwave instability will not be worsen for higher energy accelerators.

Now let us turn to transverse mode-coupling instability and consider Eq. (13.7), which we rewrite as a stability criterion

$$Z_1^{\perp}\big|_{\rm eff} \lesssim \frac{4\pi E_0 \omega_0 \nu_\beta \nu_s \tau_L}{e^2 N_b c} \ . \tag{13.46}$$

The effective impedance on the left side will be taken as the resistive-wall impedance of Eq. (13.37) multiplied by a constant. When we substitute $E_0 \sim R$, $\omega_0 \sim 1/R$, and $\nu_\beta \sim \sqrt{R}$, we obtain

$$\frac{R\sqrt{\sigma_\tau}}{b^3} \lesssim \frac{\sqrt{R}\nu_s \sigma_\tau}{N_b} \ . \tag{13.47}$$

Thus, transverse mode-coupling instability will occur when the size of the accelerator becomes bigger and bigger.

According to all the accelerator rings ever built, for electron machines, particle energy scales as $E_0 \sim \sqrt{R}$ instead. This implies that there will be no $\sqrt{R}$ on the right side of Eq. (13.47), or

$$\frac{R\sqrt{\sigma_\tau}}{b^3} \lesssim \frac{\nu_s \sigma_\tau}{N_b} \ , \tag{13.48}$$

and the instability will come at a smaller accelerator size. This may explain why electron machines are more susceptible for transverse mode-coupling instabilities. For the longitudinal microwave instability, Eq. (13.45) becomes

$$\frac{\sqrt{\sigma_\tau}}{b} \lesssim \frac{\sigma_\tau \sigma_\delta^2}{N_b \sqrt{R}} \ , \tag{13.49}$$

showing that this instability will be worsen as the size of the ring increases. For electron rings, because of the short bunch length, the longitudinal mode-coupling instability is more of interest. The stability condition for azimuthal modes $m = 2$ and 1 colliding is given by Eq. (7.10), or

$$\left|\frac{Z_0^{\parallel}}{n}\right|_{\rm ind} \lesssim \frac{4\pi \nu_s^2 \omega_0^2 \hat{\tau}^3 \beta^2 E_0}{3e^2 N |\eta|} \ . \tag{13.50}$$

Assuming again that the resistive-wall impedance dominates, we obtain

$$\frac{\sigma_\tau}{b} \lesssim \frac{\nu_s^2 \sigma_\tau^3}{N_b R^{1/2}} \ , \tag{13.51}$$

again showing that this threshold becomes more severe for a larger ring.

In Chapter 10, we show that for a proton ring, the growth rate for transverse coupled-bunch instability driven by the resistive-wall impedance should be more or less independent of the size of the accelerator ring. However, for electron rings we have $E_0 \propto \sqrt{R}$ instead. The growth rate for this instability now increases according to $\sqrt{R}$ for large electron rings. The growth time in revolution turns therefore decreases according to $R^{-3/2}$, making it much harder for the feedback damper to damp the instability in Very Large Lepton Colliders (VLLC) than in Very Large Hadron Colliders (VLHC).

13.5 Exercises

13.1. There is a simple two-particle model which gives a clear picture of transverse mode coupling [2]. Assume the head and tail particles are always separated by $\hat{z}$ for one half of a synchrotron period T_s and exchange position for the other half. Similar to Exercise 12.2, we have during $0 < s/v < T_s/2$,

$$\begin{aligned} y_1'' + k_\beta^2 y_1 &= 0 \ , \\ y_2'' + k_\beta^2 y_2 &= -\frac{e^2 N W_1(\hat{z})}{2E_0 C} y_1 \ . \end{aligned} \tag{13.52}$$

(1) Show that the solution is

$$\begin{aligned} \tilde{y}_1(s) &= \tilde{y}_1(0) e^{-ik_\beta s} \ , \\ \tilde{y}_2(s) &= \tilde{y}_2(0) e^{-ik_\beta s} - i\frac{e^2 N W_1(\hat{z})}{4E_0 C k_\beta} \left[\frac{\tilde{y}_1^*(0)}{k_\beta} \sin(k_\beta s) + \tilde{y}_1(0)\, s\, e^{-ik_\beta s} \right] \ , \end{aligned} \tag{13.53}$$

where

$$\tilde{y}_\ell = y_\ell + i\frac{y_\ell'}{k_\beta} , \qquad \ell = 1, 2 \ . \tag{13.54}$$

The term with $\sin(k_\beta s)$ in Eq. (13.53) can be dropped because $\omega_\beta T_s/2 \ll 1$. We can therefore write

$$\begin{pmatrix} \tilde{y}_1 \\ \tilde{y}_2 \end{pmatrix}_{s=vT_s/2} = e^{-i\omega_\beta T_s/2} \begin{pmatrix} 1 & 0 \\ i\Upsilon & 1 \end{pmatrix} \begin{pmatrix} \tilde{y}_1 \\ \tilde{y}_2 \end{pmatrix}_{s=0} \ , \tag{13.55}$$

where

$$\Upsilon = -\frac{\pi e^2 N W_1 v^2}{4E_0 C \omega_\beta \omega_s} \ . \tag{13.56}$$

(2) During $T_s/2 < s/v < T_s$, show that we have instead

$$\begin{aligned} y_1'' + k_\beta^2 y_1 &= \frac{e^2 N W_1(\hat{z})}{2E_0 C} y_2 \ , \\ y_2'' + k_\beta^2 y_2 &= 0 \ , \end{aligned} \tag{13.57}$$

so that for one synchrotron period,

$$\begin{pmatrix} \tilde{y}_1 \\ \tilde{y}_2 \end{pmatrix}_{s=vT_s} = e^{-i\omega_\beta T_s} \begin{pmatrix} 1 & i\Upsilon \\ 0 & 1 \end{pmatrix} \begin{pmatrix} 1 & 0 \\ i\Upsilon & 1 \end{pmatrix} \begin{pmatrix} \tilde{y}_1 \\ \tilde{y}_2 \end{pmatrix}_{s=0} \ . \tag{13.58}$$

(3) Show that the two eigenvalues are

$$\lambda_\pm = e^{\pm i\phi} , \qquad \sin\frac{\phi}{2} = \frac{\Upsilon}{2} , \tag{13.59}$$

and stability requires $\Upsilon \leq 2$. Compare the result with Eq. (13.6). Note that for a short bunch $W_1(\hat{z}) < 0$; thus Υ is positive.

13.2. In the two-particle model in Exercise 13.1, if the beam current is slightly above threshold; i.e.,

$$\Upsilon = 2 + \epsilon , \tag{13.60}$$

where $\epsilon \ll 1$, compute the complex phase ϕ of the eigenvalues $\lambda_\pm$. The growth rate is then

$$\frac{1}{\tau} = \frac{\mathcal{I}m\,\phi}{T_s} = \frac{2\sqrt{\epsilon}}{T_s} . \tag{13.61}$$

Show that for an intensity 10% above threshold, the growth time is of the order of the synchrotron period.

13.3. For longitudinal mode coupling, the coupling matrix of Eq. (13.24) can be written as, after keeping only the lowest radial modes,

$$M_{mm'} = \epsilon\omega_s A_{mm'} \tag{13.62}$$

where ϵ is given by Eq. (13.27),

$$A_{mm'} = \frac{im}{1+m}\frac{\displaystyle\int d\omega \frac{\omega_r \hat{Z}_0^{\parallel}(\omega)}{\omega}\tilde{\lambda}_{m'}(\omega)\tilde{\lambda}_m^*(\omega)}{\displaystyle\int d\omega \tilde{\lambda}_m(\omega)\tilde{\lambda}_m^*(\omega)} , \tag{13.63}$$

and $\hat{Z}_0^{\parallel}(\omega)$ has been normalized to the shunt impedance R_s.

If the coupling is not too strong, we can truncate the matrix to 2×2 for the coupling between two modes:

$$\begin{vmatrix} \dfrac{\Omega}{\omega_{s0}} - m - \epsilon A_{mm} & \epsilon A_{mm'} \\ \epsilon A_{m'm} & \dfrac{\Omega}{\omega_s} - m' - \epsilon A_{m'm'} \end{vmatrix} = 0 . \tag{13.64}$$

(1) Show that the collective frequency is given by

$$\Omega = \tfrac{1}{2}\omega_s \left[(\nu_m + \nu_{m'}) \pm \sqrt{(\nu_{m'} - \nu_m)^2 + 4\epsilon^2 A_{mm'}A_{m'm}} \right] , \tag{13.65}$$

where $\nu_k = k + \epsilon A_{kk}$, $k = m$ or m'.

(2) For simplicity, let us neglect the factor $m/(1+m)$ on the right side of Eq. (13.63). For two adjacent modes ($m' = m + 1$) that are coupled by a resonant peak, the higher-frequency mode samples mostly the capacitive part of the resonance while the lower-frequency mode samples the inductive part. Therefore $A_{mm} - A_{m'm'} > 0$. Show that $A_{mm'}A_{m'm} = -|A_{mm'}|^2$ and the threshold of instability $\epsilon_{\rm th}$ is given by

$$|\epsilon_{\rm th} A_{mm'}| = \tfrac{1}{2}|\epsilon_{\rm th}(A_{mm} - A_{m'm'}) - 1| \ . \tag{13.66}$$

The solution is different depending on whether the bunch energy is above or below transition:

$$\epsilon_{\rm th} = \frac{1}{2|A_{mm'}| + |A_{m'm'} - A_{mm}|} \qquad \text{above transition,} \tag{13.67}$$

$$|\epsilon_{\rm th}| = \frac{1}{2|A_{mm'}| - |A_{m'm'} - A_{mm}|} \qquad \text{below transition.} \tag{13.68}$$

The above shows that the threshold will be higher when the ring is below transition. In fact, the system becomes completely stable below transition if the coupling provided by the real part of the impedance is not strong enough (or $2|A_{mm'}| < |A_{m'm'} - A_{mm}|$). For this reason, it is advantageous for the ring to be of imaginary γ_t [9].

(3) When the impedance is purely reactive, the next-to-diagonal elements are zero. So we talk about coupling of two modes m and $m' = m + 2$ instead. Show that $A_{mm'}A_{m'm} = |A_{mm'}|^2$ and instability cannot occur.

(4) Show that the same conclusions in Parts (2) and (3) can be drawn when the factor $m/(1+m)$ is not neglected in Eq. (13.63), although Eqs. (13.66) and (13.68) will be slightly modified.

Bibliography

[1] R. Kohaupt, IEEE Trans. Nucl. Sci. **NS-26**, 3480 (1979); D, Rice, et al., IEEE Trans. Nucl. Sci. **NS-28**, 2446 (1981); PEP Group, Pro. 12th Int. Conf. High Energy Accel. Fermilab, 1983, p.209.

[2] R. Ruth, CERN Report LEP-TH/83-22 (1983); S. Myers, Proc. IEEE Part. Accel. Conf., Washington, 1987, p.503; B. Zotter, IEEE Trans. Nucl. Sci. **NS-32**, 2191 (1985); S. Myers, CERN Report LEP -523 (1984).

[3] V. Balakin, A. Novokhatsky, and V. Smirnov, Proc. 12th Int. Conf. High Energy Accel., Fermilab, 1983, p.11.

[4] M. Blaskiewicz, *Fast Head-tail Instability with Space Charge*, *Phys. Rev. ST Accel. Beams*, **1**, 044201 (1998).

[5] V. Danilov and E. Perevedentsev, *Strong Head-Tail Effect and Decoupled Modes in the Space-Time Domain*, *Proceedings of XVth International Conference on High Energy Accelerators*, p.1163 (Hamburg, 1992).

[6] V. Danilov and E. Perevedentsev, *Feedback system for elimination of the TMCI*, *Nucl. Instr. and Methods*, **A391**, 77 (1997).

[7] B. Chen, *The Longitudinal Collective Instabilities of Nonlinear Hamiltonian Systems in a Circular Accelerator*, Thesis, U. of Texas at Austin, May, 1995.

[8] K.Y. Ng, *Potential-Well Distortion and Mode-Mixing Instability in Proton Machines*, Fermilab Report FN-630, 1995; K.Y. Ng, *Mode-Coupling Instability and Bunch Lengthening in Proton Machines*, Proc. 1995 Particle Accelerator Conference and International Conference on High-Energy Accelerators, Dallas, Texas, May 1-7, 1995, p.2977.

[9] S.Y. Lee, K.Y. Ng, and D. Trbojevic, Phys. Rev. **E48**, 3040 (1993).